Alexandria Engineering Journal (2022) 61, 9495–9508

HOSTED BY

ELSEVIER

Alexandria University

Alexandria Engineering Journal

www.elsevier.com/locate/aej
www.sciencedirect.com

Mixed convection heat transfer utilizing Nanofluids, ionic Nanofluids, and hybrid nanofluids in a horizontal tube

Ahmed H. Abdelaziz, Wael M. El-Maghlany, Ahmed Alaa El-Din, Mohamed A. Alnakeeb *

Mechanical Engineering Department, Faculty of Engineering, Alexandria University, Egypt

Received 9 December 2021; revised 16 February 2022; accepted 1 March 2022

KEYWORDS

Nanofluids;
Hybrid nanofluids;
Ionic nanofluids;
Mixed convection;
Tube

Abstract Mixed convective heat transfer and pressure drop penalty of nanofluids flow in an isothermal horizontal tube are numerically examined in developed flow region. The study examines three types of nanofluids, simple nanofluids (*[Water]/* Al_2O_3, TiO_2, *and Cu*), Hybrid nanofluids (*[Water]/* Al_2O_3 + *Cu*), and Ionic nanofluids (*[C4mim] [NTf2]/* Al_2O_3). Richardson number is varied from 0.016 to 2, and Reynolds number is varied from 500 to 2000. The governing equations are solved numerically via the finite volume method by using the SIMPLER algorithm computer code. The computer code is validated by comparing the average Nusselt number with the experimental published data, a good agreement was observed. Performance evaluation criterion (λ) is introduced to evaluate the heat transfer enhancement gain of nanofluid usage to pressure drop penalty at different concentrations of nanoparticles. Results for nanofluids show that the maximum enhancement of the average Nusselt number is 15.5 % for Al_2O_3 with a concentration of 2% at Richardson number of 0.016. However, for hybrid nanofluids, no enhancement is noticed. Ionic nanofluid results are promising, as the Nusselt number increases significantly (by 37%) with a concentration of 2.5%. Finally, findings of various types of nanofluids investigated in the same numerical conditions are reported and compared.

1. Introduction

Nanofluids are two-phase fluids of liquid–solid mixtures that can be considered as new-generation heat-transfer fluids. Nanofluids have shown a promising future as thermal fluids for various heat transfer applications. Since solid nanoparticles with typical length scales of 1–100 nm with high thermal conductivity are suspended in the base fluid, they have been showing enhancement of effective thermal conductivity and the convective heat transfer for the base fluid, Das [1]. There are advanced concepts and practical applications of nanofluids offer fascinating heat transfer characteristics compared to con-

* Corresponding author.
E-mail address: mohamedalnakeeb@alexu.edu.eg (M.A. Alnakeeb).

Peer review under responsibility of Faculty of Engineering, Alexandria University.

https://doi.org/10.1016/j.aej.2022.03.001
1110-0168

Nomenclature

A	heat transfer surface area, m^2.
C_p	specific heat, J kg^{-1} K^{-1}.
f	coefficient of friction.
g	acceleration of gravity, m^2 s^{-1}.
Gr	Grashof number.
h	convection heat transfer coefficient, W m^{-2} K^{-1}.
k	thermal conductivity, W m^{-1} K^{-1}.
L	pipe length, m.
L*	dimensionless pipe length.
Nu_{av}	average Nusselt number.
Nu_L	local Nusselt number.
P	actual pressure, N m^{-2}.
p*	dimensionless pressure.
Pr	Prandtl number.
R	pipe inner radius, m.
Ra	Rayleigh number.
Rs	nanoparticles radius, m.
Re	Reynolds number.
Ri	Richardson number.
r	radial co-ordinate, m
r*	dimensionless radial co-ordinate.
T	temperature, K.
T_b	bulk temperature, K.
u	axial velocity component, m s^{-1}.
U_o	inlet velocity, m s^{-1}.
u*	dimensionless axial velocity.
v	radial velocity component, m s^{-1}.
v*	dimensionless radial velocity.
x	axial co-ordinate.
x*	dimensionless axial co-ordinate.

Greek symbols

α	thermal diffusivity, m^2 s^{-1}.
β	thermal expansion coefficient, K^{-1}.
θ	dimensionless temperature.
	Planck constant, J K^{-1}.
λ	performance evaluation criteria.
μ	dynamic viscosity, kg m^{-1} s^{-1}.
υ	kinematic viscosity, m^2 s^{-1}.
τ	shear stress, N m^{-2}.
ϕ	nano-particle concentration.
ρ	density, kg m^{-3}.
α	thermal diffusivity, m^2 s^{-1}.

Subscript

b	bulk
bf	base fluid.
Brownian	Brownian motion.
e	exit.
hnf	hybrid nanofluid.
i	inlet.
INF	ionic nanofluid.
nf	nanofluid.
s	solid.
w	wall.

ventional heat transfer fluids such as solar collectors [2], application of electrical transformers [3], and cooling of electronics [4]. Particle materials thermal conductivity, which can be metallic or nonmetallic such as Al_2O_3, TiO_2, *Cu*, *SiO*, *CuO* are typically order-of-magnitude higher than the base fluids. Even at low concentrations, nanoparticles can enhance the overall heat transfer significantly Bashirnezhad et al. [5]. Moreover, hybrid nanofluid is a composition of two or more nanoparticles or nano-composites synthesized and dispersed in a base fluid Babar and Ali [6]. The advantage of hybrid nanofluid in heat transfer enhancement is due to its synergistic effect compared to nanofluids containing one nanoparticle Abbas et al. [7]. It is predicted that hybrid nanofluid could offer superior thermal characteristics as compared to the base fluid and nanofluid containing single nanoparticles. Furthermore, Ionanofluids are an innovative class of new fluids, which contain suspension nanoparticles in ionic liquids (ILs). Thus, ionic nanofluids (INFs) are distinctive types of nanofluids, which consist entirely of ions and have melting point lower than 100 °C, Singh and Savoy [8]. Currently, the evolution of room-temperature ionic liquids (RTILs) has attracted great attention from researchers and industrial institutions due to their low melting temperatures which can be < 30 °C. This allows these host fluids for INFs to be used in a wide range of applications, Bakthavatchalam et al. [9]. Lee et al. [10] carried out research on four different oxide nanofluids with different volume fractions, and have concluded that the conductivity ratio of Ethelyn glycol nanofluids is higher than water for the same nanoparticles and the conductivity ratio of *CuO* is higher than Al_2O_3 for the same base fluid. Wang et al. [11] have concluded that the particle size of *CuO* is smaller than the size of Al_2O_3, which means *CuO* has higher thermal conductivity. In addition to, the agglomerate size of *CuO* particles is smaller than Al_2O_3 particles. Results of an experiment that has been held by Wen and Ding [12] on different concentrations of Al_2O_3 show that the convective heat transfer in the laminar flow regime enhanced significantly, and the enhancement increases by increasing Reynolds number. It is suggested that particle migration could be a reason for the enhancement, which results in a non-uniform distribution of thermal conductivity. Furthermore, viscosity field reduces the thermal boundary layer thickness. Esmaeilzadeh et al. [13] have studied the hydrodynamic effect and heat transfer characteristics of Al_2O_3 laminar flow and concluded that thermal conductivity rate enhancement is maximum at the inlet of the test section and decreases by increasing the distance from the inlet. Water-based TiO_2 nanofluid is studied by Colla et al. [14] to evaluate the convective heat transfer under laminar forced, and mixed flow conditions in a constant heat flux pipe. Nusselt number shows enhancement compared to the values of the base fluid. Moreover, the natural convection contribution is much weaker with nanoparticles due to their Brownian motion. Furthermore, number of researchers have been studying hybrid nanofluids experimentally and numerically. Suresh et al. [15] have presented an experimental study on a mixture of Al_2O_3 and Cu in 90:10 wt ratios respectively. Al_2O_3–$Cu/water$ hybrid nanofluids with volume concentrations from 0.1% to 2% of the base fluid. Results clarify, on one hand, that both thermal conductivity and viscosity of the prepared hybrid nanofluids are raised with the nanoparticles volume fraction, but on the other hand, the increase in viscosity is much higher than the enhancement in thermal conductivity. Measurement of thermal conductivity shows maximum enhancement of 12.11% for a volume concentration of 2% [15]. Similarly, Suresh et al. [16] have carried out an experimental study to compare friction factor between 0.1% Al_2O_3–Cu/water hybrid nanofluids and 0.1% Al_2O_3/water nanofluid. Results show that Al_2O_3–Cu/water hybrid nanofluids have a slightly higher friction factor when compared to Al_2O_3/water. Minea [17] has reviewed the challenges of hybrid nanofluids presented heat transfer characteristics of different hybrid nanofluids and numerically compared using a 3D tube model. Results show that the convective heat transfer coefficient of nanofluids increased with hybrid nanoparticle concentration and Reynolds number. The convective heat transfer coefficient of S_2 nanofluid is enhanced by 3.28 times more than base-fluid for volume concentration up to 1%. Minea and El-Maghlany [18] has carried out a numerical investigation on the effect of hybrid nanofluids in solar thermal systems. The study demonstrates an increase in average Nusselt number for the *Cu-MgO* hybrid nanofluids at a 2% volume concentration. Hence, the study has concluded that hybrid nanofluids are a strong candidate for solar energy systems, especially with solar collectors. An experimental study performed by Xie et al. [19] shows the effect of adding multi-wall carbon nanotubes (MWCNTs) to the thermophysical properties of ionic liquid-based nanofluids. Results show that the thermal conductivity of ionic nanofluids increases within the range of 1.3%–9.7% with the increasing volume concentration of MWCNTs compared to their base liquids, and slightly decreases with the increasing temperature. A numerical study is carried out by Minea and El-Maghlany [20] of an ionic liquid nanofluid. From a comparison between ionic liquid-based nanofluids and regular nanofluids, it is revealed that adding low volume concentrations of Al_2O_3 to the ionic liquid Nusselt number increases distinctively more than the water-based nanofluid. Mineaand Murshed [21] has found inconsistent and contradictory behaviour-changing of nanoparticles concentration on the viscosity of INFs. Although most of the researchers have noticed, while adding nanoparticles to the base ionic liquid, an increase in the viscosity of INFs, some numerical analyses reveal that in general, with increasing flow, the convective heat transfer coefficient increases considerably. Mixed convection of laminar flow heat transfer have been experimentally investigated by Feng and Li [22,23] for SiO_2 nanofluids in a horizontal circular tube. In addition, it is found that the augmentation in dynamic viscosity of nanofluids is far more remarkable than other thermophysical properties, and adding nanoparticles in base fluids can significantly deteriorate the convective heat transfer in the laminar mixed flow regime. Ben Mansour et al. [24] and [25] have revealed that with increasing particle volume concentration of nanofluids, Nusselt number decreases for the horizontal inclination. Furthermore, they have observed contradictory results between analytical/numerical data and experimental results regarding the heat transfer enhancement of nanofluids under buoyant forces. Jang and Choi [26] and Prasher et al. [27] have recognized that the effective thermal conductivity for nanoparticle suspensions is not simply a function of the thermal conductivity of nanoparticles added to the base fluid and/or the volume fraction of the nanoparticle. Brownian motion would allow the nanoparticles to absorb heat from the fluid surrounding them and then move to a new location and release thermal energy to the surrounding fluid at the new location Keblinski et al. [28]. The thermal diffusion of the base fluids is much faster than the Brownian diffusion of nanoparticles and, as a result, the particles could not possibly transfer heat from the hot region to the cooler region and release it into the base fluid, faster than the transfer occurring by the thermal conduction of the base fluid. As mentioned by Li and Peterson [29], Mahian et al. [30,31] it is possible that a large number of nanoparticles moving as a result of the Brownian motion could result in fluid molecules, in the immediate vicinity, to create a locally ordered micro-convection effect around each particle within the base fluid. In turn, this would enhance heat transfer. Hence, the addition of nanoparticles to a base fluid may have two possible effects: One that is the result of the higher thermal conductivity of nanoparticle material as predicted and modeled by Maxwell [32], and the other, is the result of stirring action caused by the Brownian motion of the nanoparticles. Jouybari et al. [33] conducted an experimental study on the impact of nanofluids and porous medium on flat plate solar collector thermal performance. They used nanofluids volume fractions of 0.2%, 0.4%, and 0.6% with porous medium causes increase in thermal efficiency by 8.1%. In addition, they have concluded that viscosity increases dramatically cause an undesirable increase in pressure drop. A comprehensive review of heat transfer fundamentals on transfer of nanofluids in a porous medium is carried out by Xu et al. [34] to shed some spotlights on the transport characteristics of nanofluids flowing through metal foams, advances on the forced convection and natural convection of nanofluids in porous foams and their applications.

2. Scope of the present study

From the previous review and up to the author's knowledge, the mixed convection flow coupled to the hydrodynamic behavior in tubes utilizing different nanofluids is not examined in deep detail. The receiver tube of the solar collectors needs high heat transfer coefficient fluid in the laminar flow region. In other words, the natural convection effect is found to lead to mixed convection heat transfer. The current study is on a laminar developed flow inside an isothermal circular pipe with adding different types of nano-particles to the flow, and studying their heat transfer by mixed convection and hydrodynamic behaviours by exposing them to a wide range of Richardson number from 0.016 to 2 and Reynolds number from 500 to 2000.

3. Mathematical model

The mathematical model includes the governing differential equations (conservation equations), which consists of mass, momentum, and energy conservation equations as reported by Darzi, et al. [35] in addition to boundary conditions in dimensionless form. A computational fluid dynamic (*CFD*) is used to solve the governing differential equations. The method used is the finite volume technique developed by Patankar [36]. The approaching study depends on assumptions of 2-D steady-state cylindrical co-ordinate with incompressible fluid behaviour. In addition, the Boussinesq approximation is assumed, which considers all properties including density as constant except the density term in the body force term of the equation where density variation with temperature is considered. The study is carried on a fluid flow inside an isothermal circular tube of length (L) and radius (R) at the entrance as shown in Fig. 1.

3.1. Dimensional form of governing equations

The governing equations for the current problem under consideration are based on the balance laws of mass, linear momentum, and thermal energy in two-dimensional steady-state conditions. In the light of the assumptions mentioned above, the continuity, momentum, and energy in two-dimensional equations can be written as reported by Darzi et al. [35]

$$\frac{\partial \mathrm{v}}{\partial \mathrm{r}}+\frac{\mathrm{v}}{\mathrm{r}}+\frac{\partial \mathrm{u}}{\partial \mathrm{x}}=0 \tag{1}$$

$$v\frac{\partial v}{\partial r}+u\frac{\partial v}{\partial x}=-\frac{\partial p}{\rho_{nf}\partial r}+\left(\frac{\partial^2}{\partial r^2}\left(\frac{v\mu_{nf}}{\rho_{nf}}\right)+\frac{1}{r}\frac{\partial}{\partial r}\left(\frac{v\mu_{nf}}{\rho_{nf}}\right)-\frac{v\mu_{nf}}{\rho_{nf}r^2}+\frac{\partial^2}{\partial x^2}\left(\frac{v\mu_{nf}}{\rho_{nf}}\right)\right)+ g_x\beta_{nf}(T_s-T_b) \tag{2}$$

$$u\frac{\partial u}{\partial x}+v\frac{\partial u}{\partial r}=-\frac{\partial p}{\rho_{nf}\partial x}+\left(\frac{\partial^2}{\partial r^2}\left(\frac{u\mu_{nf}}{\rho_{nf}}\right)+\frac{1}{r}\frac{\partial}{\partial r}\left(\frac{u\mu_{nf}}{\rho_{nf}}\right)+\frac{\partial^2}{\partial x^2}\left(\frac{u\mu_{nf}}{\rho_{nf}}\right)\right) \tag{3}$$

$$u\frac{\partial T}{\partial x}+v\frac{\partial T}{\partial r}=\left(\frac{\partial^2(T\alpha_{nf})}{\partial x^2}+\frac{1}{r}\frac{\partial}{\partial r}\left(r\frac{\partial(T\alpha_{nf})}{\partial r}\right)\right) \tag{4}$$

$$\tau_w=\frac{\partial(u\mu_{nf})}{\partial r}\Big]_{atwall} \tag{5}$$

3.2. Dimensionless form of governing equations

The above governing equations together with their boundary conditions are formulated in dimensionless form by using the following dimensionless parameters as follows:

$x^*=\frac{x}{d}$, $r^*=\frac{r}{d}$, $\mathrm{u}^*=\frac{\mathrm{u}}{\mathrm{U_o}}$, $\mathrm{v}^*=\frac{\mathrm{v}}{U_o}$, $\mathrm{v}^*=\frac{\mathrm{v}}{U_o}$, $p^*=\frac{p}{\rho_{bf}U_o^2}$, $\theta=\frac{T-T_w}{T_i-T_w}$, $\tau^*=\frac{\tau_w}{\rho_{bf}U_o^2}$, $\upsilon_{nf}=\frac{\mu_{nf}}{\rho_{nf}}$, $Pr=\frac{\mu_{bf}C_p}{k_{bf}}$, $Re=\frac{\rho_{bf}\mathrm{U_o d}}{\mu_{bf}}$, $Gr=\frac{g\beta(T_s-T_b)d^3}{\upsilon_{bf}^2}$, $Ra=GrPr$, $Ri=\frac{Gr}{Re^2}$

By applying the previously mentioned dimensionless parameters and groups on the dimensional equations, dimensionless equations can emerge in terms of continuity, momentum, and energy equations as follow:

$$\frac{\partial \mathrm{v}^*}{\partial r^*}+\frac{\mathrm{v}^*}{r^*}+\frac{\partial \mathrm{u}^*}{\partial x^*}=0 \tag{6}$$

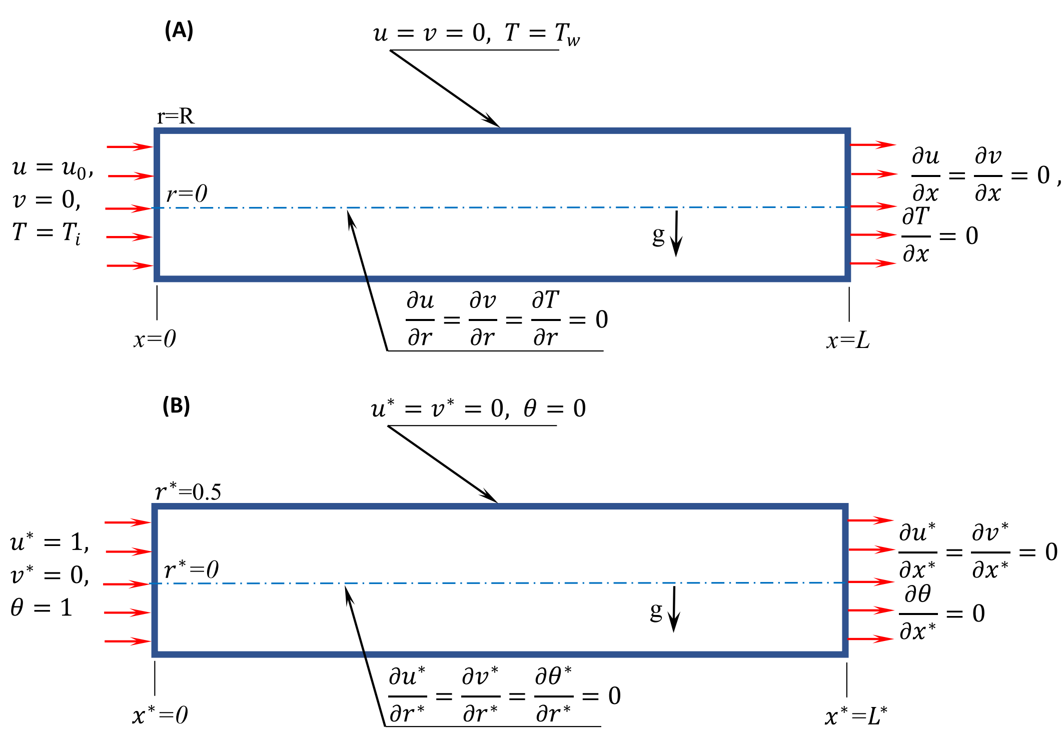

Fig. 1 Schematic diagram of the present Problem with dimensional and dimensionless boundary conditions.

$$v^*\frac{\partial v^*}{\partial r^*}+u^*\frac{\partial v^*}{\partial x^*}=-\frac{\rho_{bf}\partial p^*}{\rho_{nf}\partial r^*}+\frac{1}{Re}\left(\frac{\partial^2}{\partial r^{*2}}\left(\frac{v^*\upsilon_{nf}}{\upsilon_{bf}}\right)+\frac{1}{r^*}\frac{\partial}{\partial r^*}\left(\frac{v^*\upsilon_{nf}}{\upsilon_{bf}}\right)-\frac{v^*\upsilon_{nf}}{\upsilon_{bf}r^{*2}}+\frac{\partial^2}{\partial x^{*2}}\left(\frac{v^*\upsilon_{nf}}{\upsilon_{bf}}\right)\right)+\frac{(\rho\beta)_{nf}}{(\rho\beta)_{bf}}Ri\theta \quad (7)$$

$$u^*\frac{\partial u^*}{\partial x^*}+v^*\frac{\partial u^*}{\partial r^*}=-\frac{\rho_{bf}\partial p^*}{\rho_{nf}\partial x^*}+\frac{1}{Re}\left(\frac{\partial^2}{\partial r^{*2}}\left(\frac{u^*\upsilon_{nf}}{\upsilon_{bf}}\right)+\frac{1}{r^*}\frac{\partial}{\partial r^*}\left(\frac{u^*\upsilon_{nf}}{\upsilon_{bf}}\right)+\frac{\partial^2}{\partial x^{*2}}\left(\frac{u^*\upsilon_{nf}}{\upsilon_{bf}}\right)\right) \quad (8)$$

$$u^*\frac{\partial\theta}{\partial x^*}+v^*\frac{\partial\theta}{\partial r^*}=\frac{1}{PrRe}\left(\frac{\partial^2}{\partial x^{*2}}\left(\frac{\theta\alpha_{nf}}{\alpha_{bf}}\right)+\frac{1}{r^*}\frac{\partial}{\partial r^*}\left(r^*\frac{\partial}{\partial r^*}\left(\frac{\theta\alpha_{nf}}{\alpha_{bf}}\right)\right)\right) \quad (9)$$

$$\tau^*=\frac{1}{Re}\frac{\partial}{\partial r^*}\left(\frac{u^*\mu_{nf}}{\mu_{bf}}\right) \quad (10)$$

The boundary condition in dimensionless form can be represented as the following:

at $x^*=0$:	$u^*=1$, $v^*=0$, $\theta=1$
at $x^*=L^*$:	$\frac{\partial\theta}{\partial x^*}=\frac{\partial u^*}{\partial x^*}=\frac{\partial v^*}{\partial x^*}=0$
at $r^*=0.5$:	$u^*=v^*=0 and \theta=0$
at $r^*=0$:	$\frac{\partial u^*}{\partial r^*}=\frac{\partial v^*}{\partial r^*}=\frac{\partial\theta}{\partial r^*}=0$

3.3. Nanofluids properties

The thermophysical properties of pure water, Al_2O_3, TiO_2, and Cu are selected from [37] as shown in Table 1. Thermophysical properties of nanofluids can be calculated from equations and correlations from the model that was proposed by Ghasemi and Aminossadati [37].

$$\text{VolumeFraction}\phi=\frac{Volumeofnanoparticles}{TotalVolumeofSolution} \quad (11)$$

$$\text{Density}\rho_{nf}=(1-\phi)\rho_{bf}+\phi\rho_s \quad (12)$$

$$\text{Heatcapacitance}(\rho C_p)_{nf}=(1-\phi)(\rho C_p)_{bf}+\phi(\rho C_p)_s \quad (13)$$

$$\text{ThermalExpansionCoefficient}(\rho\beta)_{nf}=(1-\phi)(\rho\beta)_{bf}+\phi(\rho\beta)_s \quad (14)$$

$$\text{Thermaldiffusivity}\alpha_{nf}=\frac{k_{nf}}{(\rho C_p)_{nf}} \quad (15)$$

$$\text{Viscosity}\mu_{nf}=\mu_{static}+\mu_{Brownian}=\frac{\mu_{bf}}{(1-\phi)^{2.5}}+5\text{x}10^4\beta\phi\rho_{bf}\sqrt{\frac{A\ddot{T}}{2\rho_s R_s}}f(T,\phi) \quad (16)$$

$$\text{ThermalConductivity}k_{nf}=k_{static}+k_{Brownian}=k_{bf}[\frac{(k_s+2k_{bf})-2\phi(k_{bf}-k_s)}{(k_s+2k_{bf})+\phi(k_{bf}-k_s)}]+5\times10^4\beta\phi(\rho C_p)_{bf}\times\sqrt{\frac{A\ddot{T}}{2\rho_s R_s}}f(T,\phi) \quad (17)$$

Where $k=1.3807\text{x}10^{-23}$ (J/K)

$$\beta=0.0137(100\phi)^{-0.8229}\text{for}\phi<1\% \quad (18)$$

$$\beta=0.0011(100\phi)^{-0.7272}\text{for}\phi>1\% \quad (19)$$

$$f(T,\phi)=(-6.04\phi+0.4705)T+(1722.3\phi-134.63) \quad (20)$$

for $1\% \le \phi \le 4\%$ and 300 K $< T < 325K$

Hybrid and ionic nanofluid thermophysical properties are far more complex than simple nanofluids which are preferred to use the experimental published data of Mehryan et al. [38], Paul et al. [39]. For hybrid nanofluids (Water / Al_2O_3 + Cu), the thermophysical properties are selected from [38] as illustrated in Table 2. Suresh et al [15] carried out experimental work to reveal the real thermal properties of hybrid nanofluids by following specific steps. Nanocrystalline alumina–copper hybrid (Al_2O_3-Cu) powder was prepared by a thermochemical synthesis method which consists of the following stages: spray-drying, oxidation of precursor powder, reduction by hydrogen, and homogenization. The average grain size of the hybrid particles was calculated to be 17 nm. Al_2O_3–Cu/water hybrid nanofluids with volume fractions from 0.1 to 2% were prepared using the two-step method. Nanofluid with a required volume concentration was prepared by dispersing a specified amount of Al_2O_3–Cu nanoparticles in deionized water with Sodium Lauryl Sulphate (SLS) as dispersant by using an ultrasonic vibrator (Lark, India) generating ultrasonic pulses of 180 W at 40 kHz.

Ionic nanofluids properties are chosen from the experimental study of Paul et al. [39] as shown in Table 3. Nanoparticles enhanced ionic liquids (NEILs) with volume concentration of 0.18%, 0.36%, and 0.9% were prepared by 1-butyl-3-methylimidazolium bis[(trifluoromethyl)sulfonyl]imide, ($[C_4mim][NTf_2]$) IL with Al_2O_3 nanoparticles. Aluminium oxide (Al_2O_3) nanoparticles were dispersed in the base IL by using vortex mixture. NEILs were processed for around 90 min in the votexture to break possible aggregations of nanoparticles.

Table 1 The thermophysical properties of base fluid and nanoparticles [37].

Thermophysical properties	Pure Water	Al_2O_3	TiO_2	Cu
ρ (kg/m^3)	997.1	3970	4250	8933
C_p (J/kg K)	4179	765	6862	385
K (W/m K)	0.613	40	8.9538	400
$\beta\times10^{-5}$ (K^{-1})	21	0.85	0.9	1.67
$\mu\times10^{-4}$ (kg/m s)	8.9	–	–	–

Table 2 The thermophysical properties of hybrid nanofluids [38].

Thermophysical properties	Al_2O_3 + Cu / Water	
ϕ	*1%*	*2%*
ϕ_{Al2O3}	*0.962 %*	*1.9241 %*
k (W/m K)	*0.657*	*0.685*
$\mu \times 10^{-4}$ (kg/m s)	16.02	19.35
ρ (kg/m^3)	1030.1	1060.32
$(\rho\ C_p)_{hnf} \times 10^6$ (J/m^3 K)	4.16	4.144
$(\rho\ \beta)_{hnf} \times 10^{-2}$ (kg/m^3 K)	20.76	20.59

3.4. Nusselt number, friction coefficient, and performance evaluation criteria

The local Nusselt number is given by:

$$Nu_{Local} = \frac{\frac{\partial}{\partial r^*}\left(\frac{\theta k_{nf}}{k_{bf}}\right)\rfloor_{r^*=0.5}}{\theta_w - \theta_b} \tag{21}$$

Where θ_b is the bulk temperature through a pipe at a given section and given by:

$$\theta_b = \left(\frac{\int_0^{0.5} u^*\theta dr^*}{\int_0^{0.5} u^* dr^*}\right)_{x^*} \tag{22}$$

The average Nusselt number is given by:

$$Nu = \frac{1}{L^*}\int_0^{L^*} Nu_{Local} dx^* \tag{23}$$

As the force due to shear stress equals that from drag force so that the friction coefficient can be calculated as.

$$f = \frac{8\tau_w}{\rho u^2} \tag{24}$$

The friction coefficient in dimensionless form is given by:

$$f = 8\tau^* = \frac{8}{Re}\frac{\partial}{\partial r^*}\left(\frac{u^*\mu_{nf}}{\mu_{bf}}\right) \tag{25}$$

Performance evaluation criteria of a certain hydro-dynamic system of fluid flow can be defined as a ratio between enhancements in heat transfer to fluid flow friction effect (λ) as it was mentioned by Hussein et al [40]. So λ can be estimated as

$$\lambda = \frac{\frac{Nu}{Nu_{\phi=0}}}{\left(\frac{f}{f_{\phi=0}}\right)^{1/3}} \tag{26}$$

3.5. Solution procedures

The previous governing equations are numerically solved by Fortran-code program using the finite volume method developed by Patankar [36]. The technique is built on the discretization of the domain using the central difference in space. The pressure and velocity fields are coupled, which was conducted by SIMPLE Algorithm. The discretization grid is uniform in the circumferential direction and non-uniform in the other two directions, discretization equations were solved by the GausseSeidel method. The iterations (sweeping the computational domain along the radial and circumferential directions) were made using a line-by-line system, which is a combination of the direct method and the resulting Tri Diagonal Matrix Algorithm (TDMA) that can be solved easily by known steps. The convergence of the solution is established by the change in average Nusselt number through 2500 iterations to achieve a difference of < 0.01% between two consecutive values. A grid study is made as shown in Fig. 2. The grid size of (400 nodes in the axial direction and 40 nodes in the radial direction) is sufficient. The average Nusselt number starts to converge after the 2000 iterations. Therefore, it would be sufficient to choose 2500 iterations as displayed in Fig. 3.

3.6. Numerical code Validation

In order to demonstrate the validity and the precision of the numerical code, the Nusselt number has been compared with the corresponding experimental published results of Hekmatipour et al. [41]. They have experimentally studied the mixed convection heat transfer of oil-copper oxide (HTO-CuO) nanofluid laminar flow in isothermal horizontal tubes. Also, they studied the effect of adding solid particles of copper oxide with the average size of 40 nm and the purity of 99% to oil (HTO) with mass concentrations of 0.5%, 1%, and 1.5% on the average Nusselt number with a variation of Rayleigh number from 20,000 to 140000. The Nusselt number of mixed convection is in good agreement with the corresponding experimental published results, where the maximum deviation was about 8.6 % at Ra(D/L) of 68,000 and nanofluid mass concentration of 1.5 %, which is accepted over the entire range as shown in Fig. 4.

4. Results and discussion

The present study results can be classified according to the type of added nanoparticles; nanofluids, hybrid nanofluids, and ionic nanofluids. To explain the results properly, the behavior of thermophysical properties of the three types of nanofluids

Table 3 The thermophysical properties of ionic nanofluids and its base fluid [39].

Thermophysical properties	*[C4mim] + [NTf$_2$] + Al$_2$O$_3$*			
ϕ	0%	0.5%	1%	2.5%
ρ (kg/m^3)	1386	1390	1425	1453
C_p (J/Kg K)	1744	2040	2270	2600
k (W/m K)	0.123	0.127	0.132	0.135
$\mu \times 10^{-2}$ (Kg/m s)	1.62	1.7	2	3.9
$\beta \times 10^{-4}$ (K^{-1})	6.48	6.45	6.42	6.32

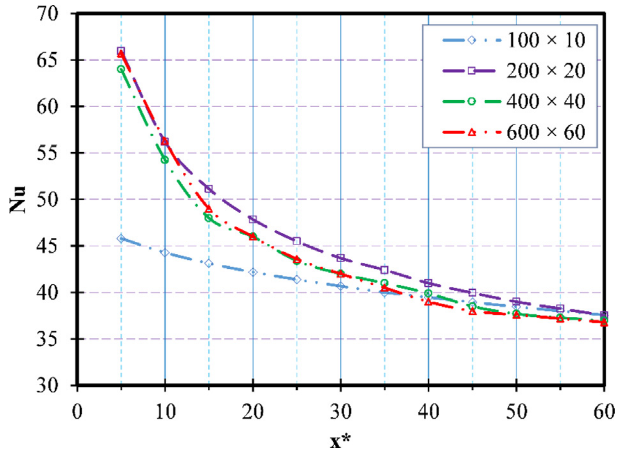

Fig. 2 Grid independence test.

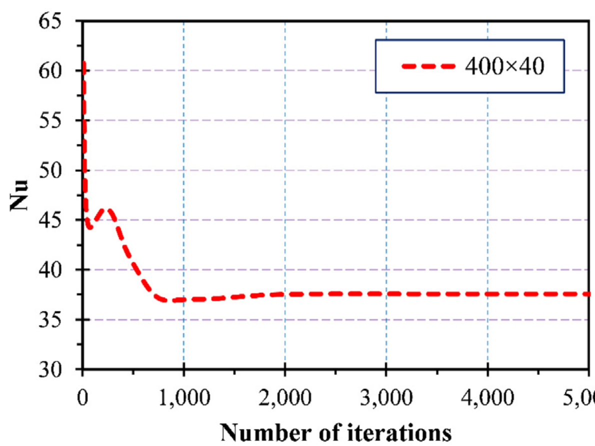

Fig. 3 Number of required iterations.

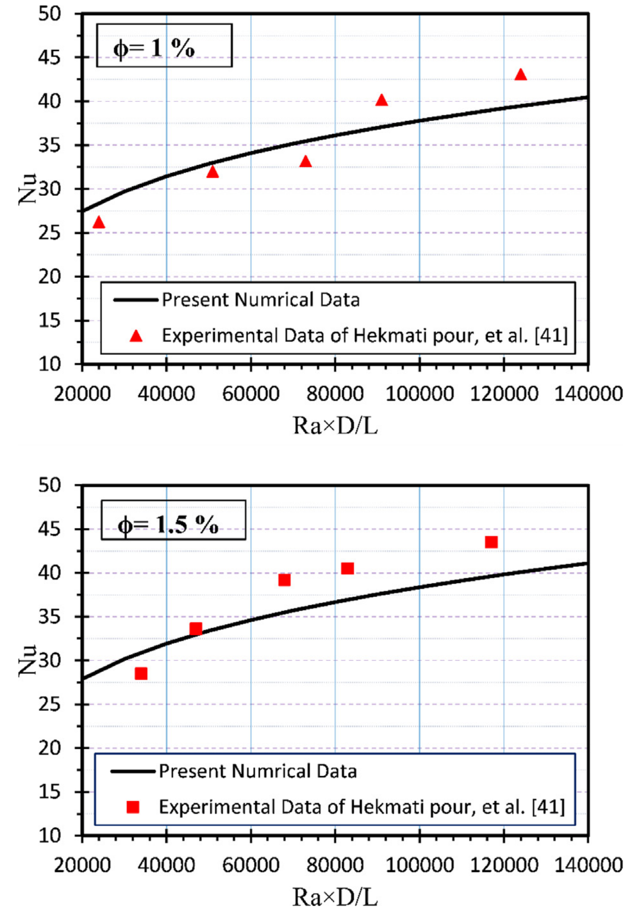

Fig. 4 Validation for average Nusselt number with experimental data of [41].

should be understood correctly with respect to flow speed and nanoparticles concentration. In natural convection heat transfer thermal conductivity (k), thermal volumetric expansion (β), and dynamic viscosity (μ) are the main three parameters that affect thermal and flow field behavior. The natural convection is affected by the ratio between the buoyancy force and the viscous force. Buoyancy force mainly depends on the thermal volumetric expansion, and viscous force depends on viscosity. Thus, the increase in thermal volumetric expansion and decrease in dynamic viscosity enhances the natural convection mechanism due to the potential of the weight effect of the Richardson number term in Eq. (7) and vice versa. The increase in thermal conductivity, which is the main effect of the addition of the nanoparticles, enhances the Nusselt number. As the present study focuses on mixed convection, in addition to natural convection which has been explained previously, forced convection behavior should be considered as well. Reynolds number plays a critical role not only to determine the type of flow but also in the resulted friction, which can be presented by the friction coefficient (f). Consequently, flow speed and nanoparticles concentration draw the enhancement map of the Nusselt number at the same Richardson number. Hence, both aspects should be studied carefully to determine the suitable type of fluid for a certain application that depends on their performance evaluation criteria (λ). According to the above clarification, the experimental thermophysical properties of the hybrid nanofluids and Iona-nofluid strongly affect the heat transfer results. Therefore, the results would be adequately discussed.

4.1. Nanofluids

Three different nanoparticles would be added to the base fluid (water), Al_2O_3, TiO_2 and Cu respectively, to form three different nanofluids with different concentrations of 0.5%, 1%, and 2%. Thermophysical properties equations of nanofluids, as selected from Ghasemi and Aminossadati [37] with considering the Brownian effect, are shown in Table 1.

A wide range of Richardson number is studied to represent the variation of Nusselt number, and its ratio on both pure water and nanofluids. This effect could be illustrated in Fig. 5. It is shown that at low Richardson number, Nusselt number value of nanofluids is greater than of pure water. However, by increasing the Richardson number, the Nusselt number value of nanofluids decreases till it becomes less than pure water. The natural motion of nanoparticles could explicate this strange behavior since Richardson number values are low flow could be assumed pure forced so random particle migration could be neglected compared to fluid flow momentum and the enhancement of Nusselt number due to the enhancement in the overall thermal conductivity of nanofluids. On the other hand, at high values of Richardson number natural convection tends to have a major role in heat transfer. In addition to considering Brownian motion, it has negatively contributed to heat transfer enhancement, which agrees with Wen and Ding [12]. From another point of view, the ratio of Nusselt number could interpret the small difference between nanofluids as shown in Fig. 5. In contrary to what has been expected, *Cu* nanoparticles should give better results than Al_2O_3 and TiO_2, as the thermal conductivity of *Cu* is an order of magnitude higher than Al_2O_3. However, the density of *Cu* is almost twice the density of Al_2O_3, while taking into consideration the mixed convection effect which depends on the free motion of particles. So, by having a greater density, the buoyancy force effect would be decreased then the free motion would be reduced, which would lead to less heat transfer ability compared to Al_2O_3 and TiO_2. The effect of changing *Re* on friction coefficient is displayed in Fig. 5.

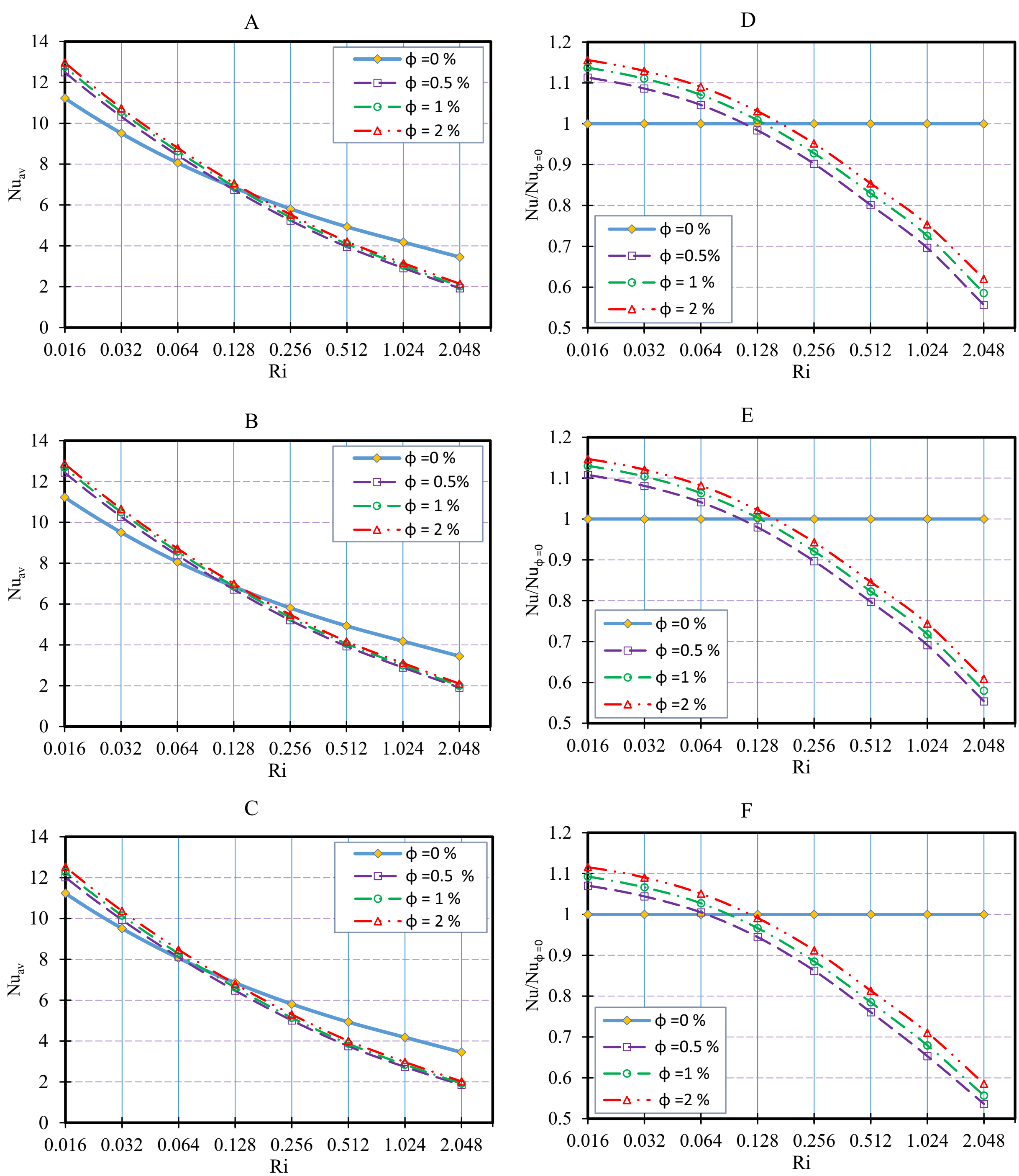

Fig. 5 Average Nusselt number versus Richardson number and $\phi = 0.5, 1, 2$ % at different nanoparticles (A-D) Al_2O_3, (B-E) TiO_2, *and* (C-F) *Cu*.

The results show that adding nanoparticles does not significantly change the friction coefficient over a wide range of Reynolds number. However, at low Reynolds number, strange behavior of nanofluids is observed, as it tends to increase then it reverses its direction to decrease again as illustrated in Fig. 6. This could be explained that the presence of second flow has a critical role in the determination of value and direction of friction on the fluid flow as a result of Brownian motion of nanofluid particles, especially in low Reynolds number. In addition, a slight increase in friction of nanofluids over pure water is noticed at a high Reynolds number. This is due to a slight increase in the dynamic viscosity of nanofluids.

By combining the previous two parameters; Nusselt number and friction coefficient, the performance evaluation criteria could be emerged. It is observed that (λ) decreases dramatically at low Reynolds number then starts to be constant. This behavior can be explained by the effect of decreasing Nusselt number is canceled by the increase in friction. Moreover, it can be concluded that the efficiency of Al_2O_3 and TiO_2 is

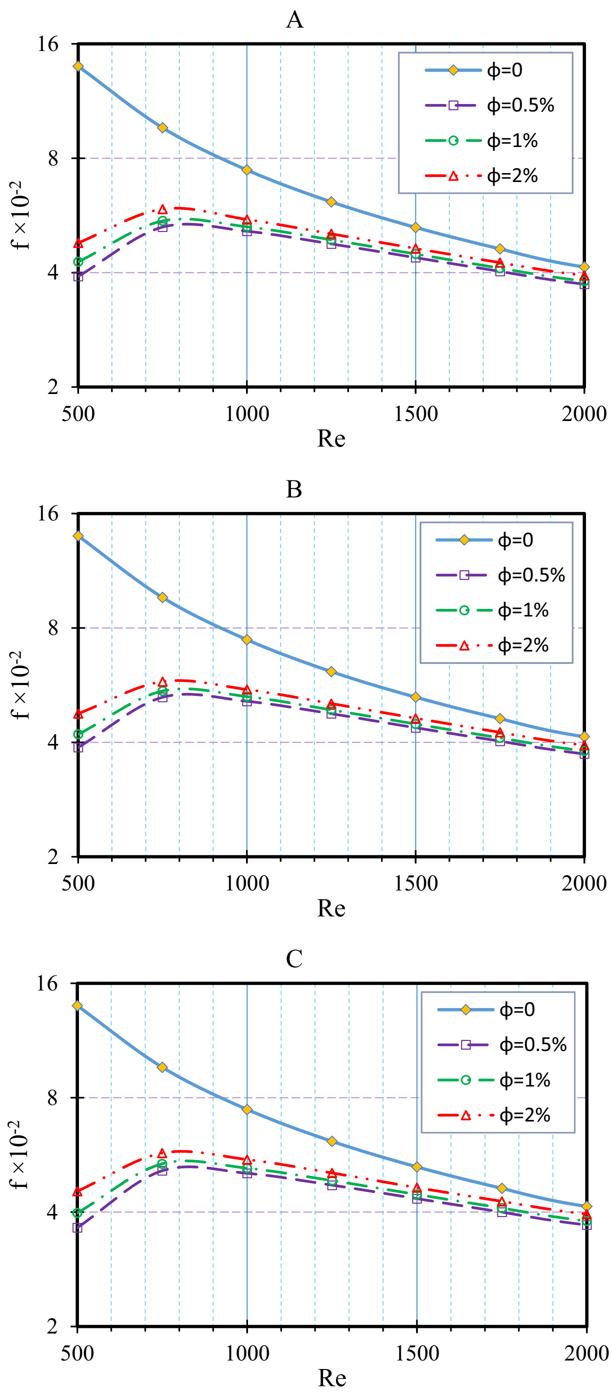

Fig. 6 Friction coefficient versus *Re* for ϕ = 0.5, 1, 2 % at different nanoparticles *(A)* Al_2O_3, *(B)* TiO_2, and *(C)* *Cu*.

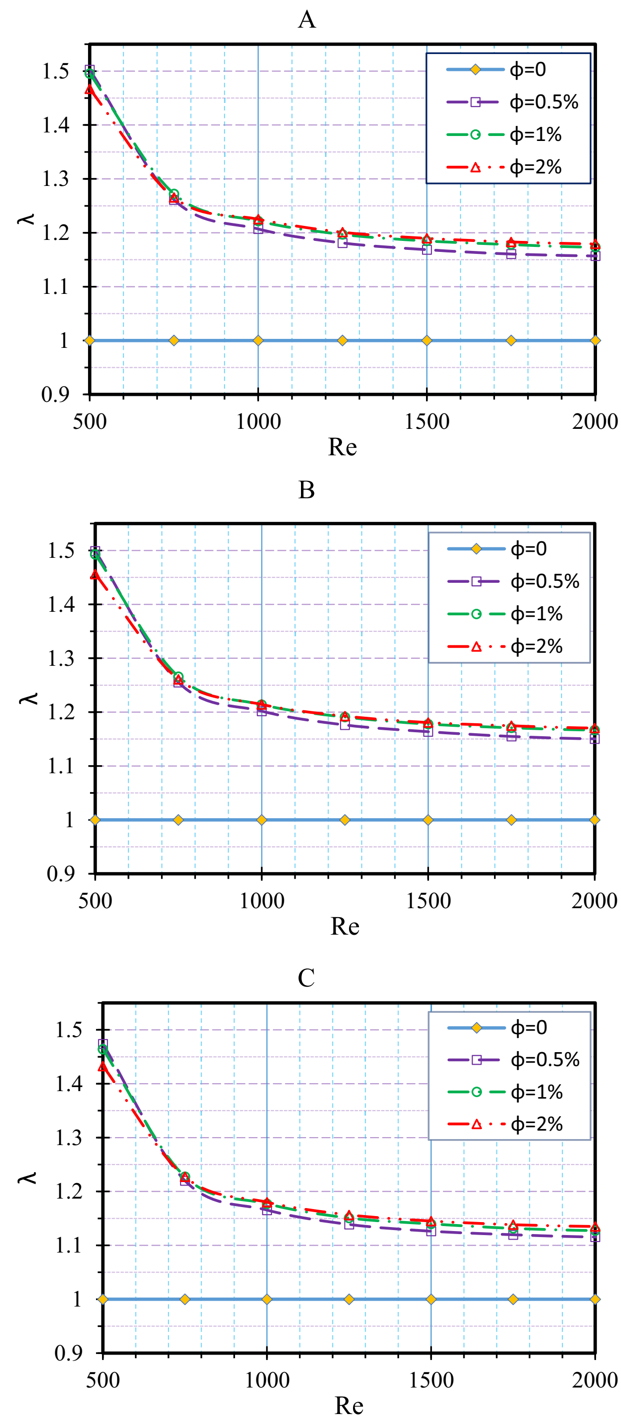

Fig. 7 Performance evaluation criteria versus *Re* for ϕ = 0.5, 1, 2 % at different nanoparticles *(A)* Al_2O_3, *(B)* TiO_2, and *(C)* *Cu*.

higher than *Cu* by 4.5% as shown in Fig. 7. This is due to the higher Nusselt number of the first two nanofluids than the last one with similar friction behavior. Finally, all the nanofluids positively affected the Nusselt number by increasing volumetric concentration at low *Ri* especially Al_2O_3 nanofluid, which has the best thermal performance over the other nanofluids.

4.2. Hybrid nanofluids

For the hybrid nanofluids, Aluminum oxide particles would be mixed with copper particles in water as base fluid with the ratios mentioned in Table 2, with two concentrations of 1% and 2%. The experimental thermophysical properties are given in the study by Mehryan et al. [38], and its proposed model is applied. The effect of adding hybrid nanoparticles to pure water would be studied on the Nusselt number ratio and pressure drop in addition to the efficiency of heat transfer for each concentration. As observed from Fig. 8, the Nusselt number ratio of hybrid nanofluids is less than pure water over the wide range of Richardson number, which can be referred to as the excessive increase in the dynamic viscosity. The pressure drop in (Al_2O_3 + *Cu* / water) is much higher than pure water, for which 1% and 2% are 5 times and 8 times respectively of pure water, which agrees with [15]. This tremendous friction effect can be explained as the higher dynamic viscosity of hybrid nanofluid Fig. 9. As it can be expected, pressure drop has a deep impact on heat transfer efficiency, in addition to a lower Nusselt number, the overall efficacy of hybrid nonfluid is much less than that of pure water Fig. 10. Adding hybrid nanofluids negatively affected the *Nu* in addition, the high dynamic viscosity strongly increases the pressure drop of the hybrid nanofluids.

4.3. Ionic Nanofluids

The experimental thermophysical properties of IoNanofluids are obtained by adding three different concentrations of Al_2O_3 nanoparticles (0.5, 1, and 2.5%) to the base fluid ([*C4mim*] [NTf_2]), which are selected from Darzi et al. [29] as shown in Table 3. The effect of adding different concentrations of nanoparticles in the ionic base fluid would be studied by varying Richardson number, and show its effect on Nusselt number ratio Fig. 11 in addition to studying pressure drop ratio and thermal efficiency with changing Reynold number Fig. 12, Fig. 13.

It is noticed from Fig. 11 that the average enhancement of ionic nanofluids Nusselt number ratio is 8.8 %, 17.9 %, and 30 % as the concentration of nanoparticles increases by 0.5%, 1%, and 2.5% respectively, compared to the Ionic fluid. By a closer look at the higher Richardson number, it is observed that, as much as the Richardson number increases, the enhancement in the Nusselt number slightly increases. This is due to the major role played by natural convection in heat transfer enhancement as mentioned by Minea and El-Maghlany [18].

Moreover, Fig. 12 shows the effect of the pressure drop ratio regarding the increase in Reynolds number. It is noticed that by adding 2.5% of Al_2O_3 to ionic fluid, the friction significantly increases due to a sharp increase in dynamic viscosity of ionic nanofluid with ϕ = 2.5 % that leads to an increase of pressure drop to 12 times its base fluid which agrees with

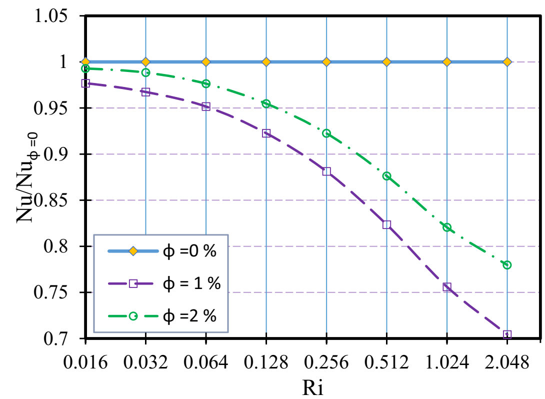

Fig. 8 Nusselt number ratio of hybrid nanofluids (*[Water]/ Al_2O_3 + Cu*).

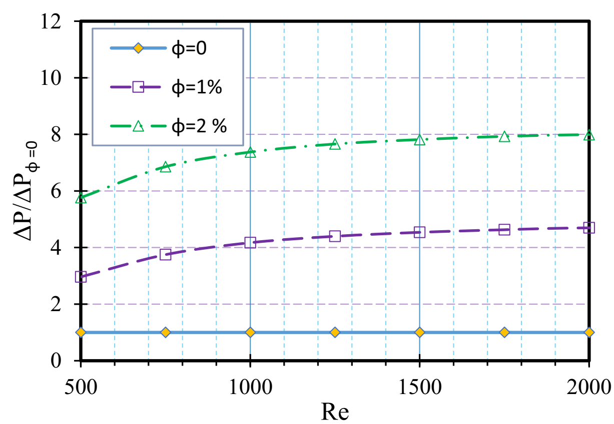

Fig. 9 Pressure drop ratio of hybrid nanofluid ([Water]/ Al2O3 + Cu).

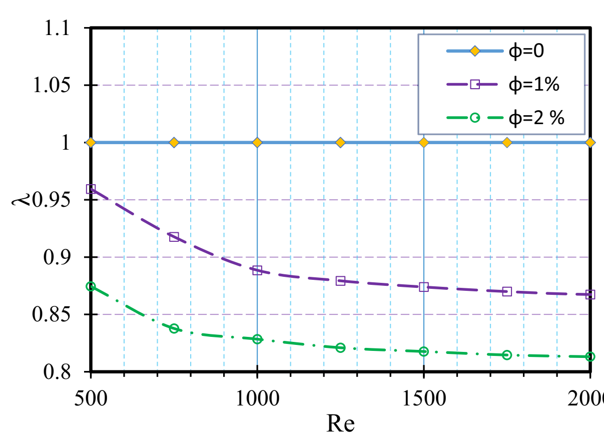

Fig. 10 Performance evaluation criteria of hybrid nanofluids. *([Water]/ Al2O3 + Cu)*.

Mehryan et al. [39] findings. In the case of ionic nanofluids Fig. 13, it appears that the Performance evaluation of ϕ = 0.5% and ϕ = 1% is better than pure ionic fluid by 5 %. However, despite the superiority of ionic nanofluid of ϕ = 2.5% in the enhancement of heat transfer, it shows less effi-

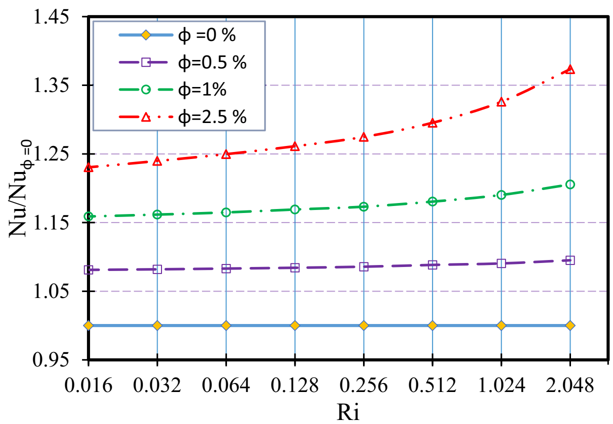

Fig. 11 Nusselt number ratio of ionic nanofluids *([C4mim] [NTf₂]/ Al₂O₃)*.

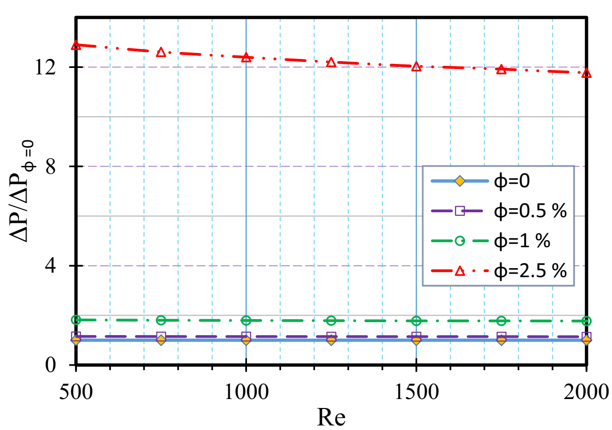

Fig. 12 Pressure drop ratio of ionic nanofluids *([C4mim] [NTf₂]/ Al₂O₃)*.

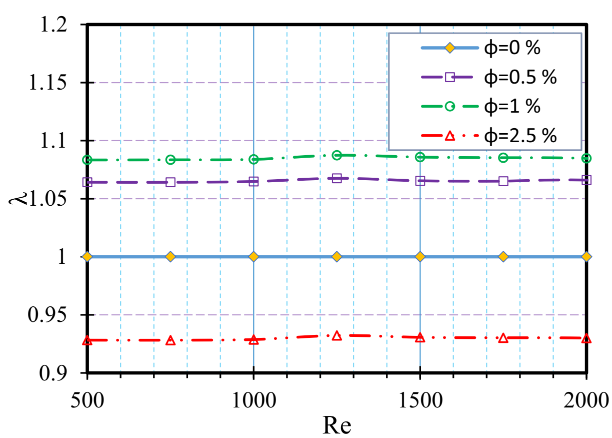

Fig. 13 performance evaluation criteria of ionic nanofluids. *([C4mim] [NTf₂]/ Al₂O₃)*.

ciency than other concentrations (10% less than pure ionic fluid). This drawback could be interpreted as the high friction significantly impacting the overall heat transfer efficiency of

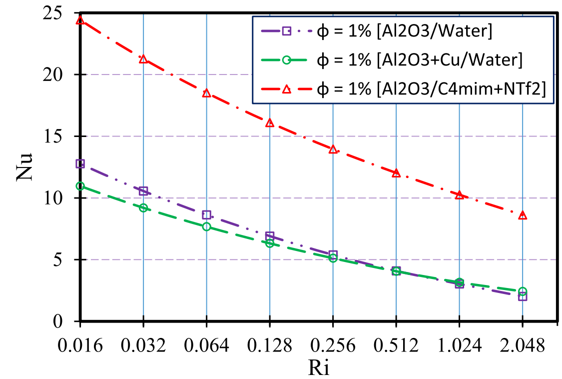

Fig. 14 Comparison of Nusselt number between three types of nanofluids; Simple *(Al₂O₃/ Water)*, Hybrid *(Al₂O₃ + Cu / water)*, and Ionic *(Al₂O₃ /C4mim- NTf₂)*.

ionic nanofluid. Finally, increasing of nanoparticles concentration in ionic liquids improves the heat transfer but the excess of it (2%) will significantly boost the friction effect and diminish the performance evaluation criteria.

4.4. Comparison between the three types of nanofluids

Finally, to sum up, the effect of adding nanoparticles to different base fluids on heat transfer characteristics and friction losses it is required to compare their thermo-hydraulic performance under the same conditions. Therefore, a concentration of 1% has been chosen as a reference for each type of nanofluids, hence it could show the disparity between different nanofluids from the points of Nusselt number, Nusselt number ratio, friction coefficient, pressure drop ratio, and thermal efficiency. It can be deduced from Fig. 14 that ionic nanofluids are superior to nanofluids and hybrid nanofluids in terms of Nusselt number by almost double its value as a result of their high heat capacity and thermal conductivity. Similarly, in Fig. 15, the ratio of Nusselt number enhancement of ionic nanofluid over its base fluid is better than the raise served by nano and hybrid nanofluids for the same concentration. At higher ranges

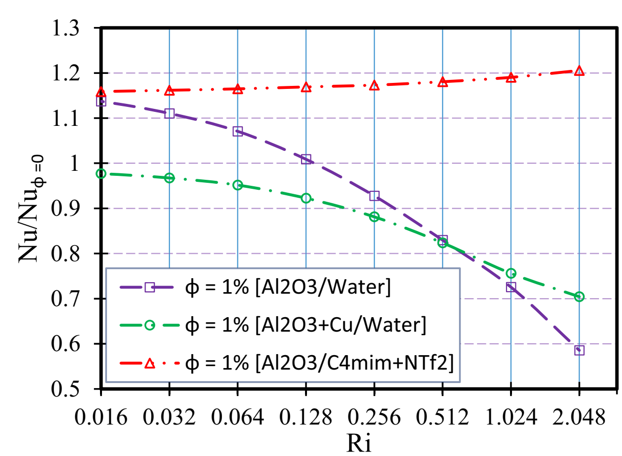

Fig. 15 Comparison of Nusselt number ratio between three types of nanofluids; Simple *(Al₂O₃/ Water)*, Hybrid *(Al₂O₃ + Cu / water)*, and Ionic *(Al₂O₃ /C4mim- NTf₂)*.

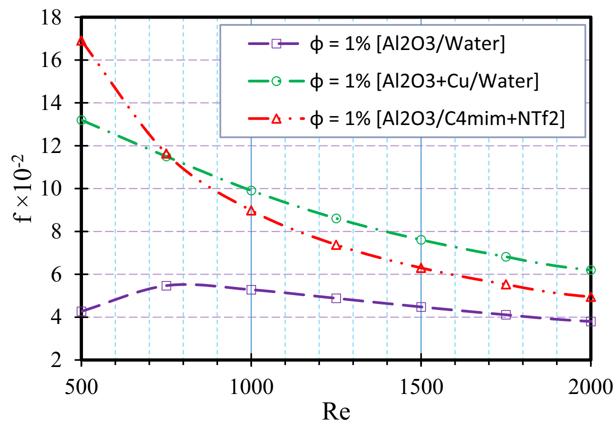

Fig. 16 Comparison of friction factor between three types of nanofluids; Simple $(Al_2O_3/\ Water)$, Hybrid $(Al_2O_3 + Cu\ /\ water)$, and Ionic $(Al_2O_3\ /C4mim\text{-}\ NTf_2)$.

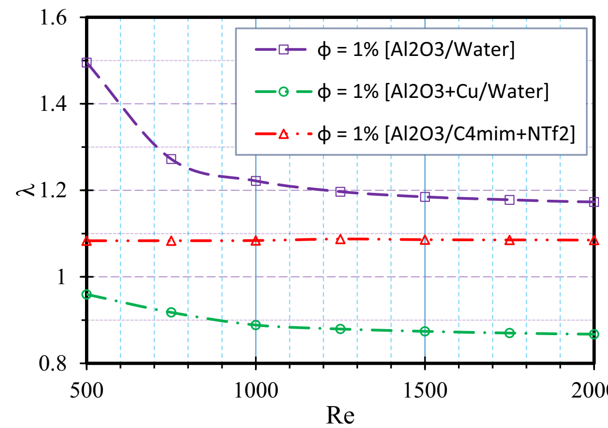

Fig. 18 Comparison of Thermal heat efficiency between three types of nanofluids; Simple $(Al_2O_3/\ Water)$, Hybrid $(Al_2O_3 + Cu\ /\ water)$, and Ionic $(Al_2O_3\ /C4mim\text{-}\ NTf_2)$.

(Ri > 0.5) Nusselt number of ionic nanofluids is enhanced by 19 % to its base fluid. On the contrary, the nanofluid Nusselt number is decreased by 30% of its base fluid at Ri = 2. On the other hand, hybrid nanofluids have higher friction loss and pressure drop due to the rapid increase in dynamic viscosity only by adding 1% of hybrid nanoparticles over the pure water as shown in Fig. 16. In the low Reynolds number region (Re = 500) the friction factor of ionic nanofluids is higher than the friction factor of hybrid until Re = 750 when the friction factor of ionic nanofluids started to decrease to be less than hybrid nanofluids. On the other side, the friction factor of nanofluids is less than both over the range of Reynolds number. Accordingly, the difference in pressure drop ratio can be shown in Fig. 17 nanofluids and hybrid nanofluids show a rapid increase in pressure drop at Re < 1000 and a more steady increase at Re > 1000. Besides ionic nanofluids shows steady pressure drop performance along with the range of 500 < Re < 2000. From another point of view, nanofluid performance evaluation criterion matches both higher heat transfer availability with accepted friction losses as displayed in Fig. 18 with an average improvement of 20 % for Re > 1000. For ionic performance evaluation criteria is improved by only 8 %, but hybrid nanofluid efficiency is decreased by 13% of its base fluid. It is highly recommended to utilize the nanofluids at low fluid speeds (Re < 1000) and to apply ionic nanofluids with the application that requires higher thermal performance regardless of the resulting pressure drop penalty.

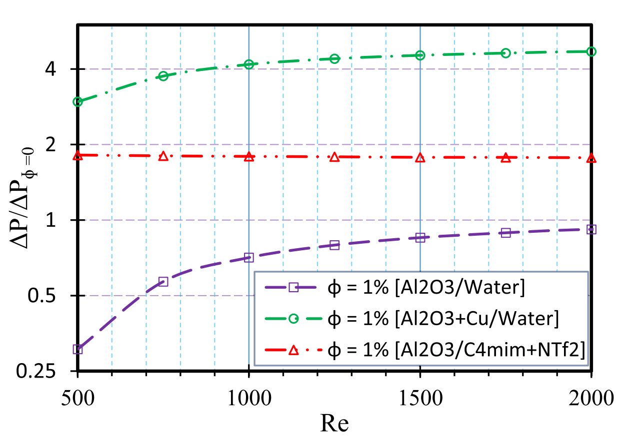

Fig. 17 Comparison of pressure drop ratio between three types of nanofluids; Simple $(Al_2O_3/\ Water)$, Hybrid $(Al_2O_3 + Cu\ /\ water)$, and Ionic $(Al_2O_3\ /C4mim\text{-}\ NTf_2)$.

5. Conclusion

A comparative numerical study on three types of nanofluids; simple, hybrid, and ionic was performed by changing their volumetric concentration (ϕ) with the variation of Richardson number and Reynolds number to determine their effect of mixed convection mechanism on heat transfer enhancement and hydrodynamics of nanofluids. The effect of particle Brownian motion and fluid thermal diffusion on heat transfer behaviour is considered. The following findings were reviled from the detailed comparison that is implemented between different types of nanofluids.

- Three nanoparticles are added to pure water to form several nanofluids; Al_2O_3, TiO_2, and Cu with different concentrations (0.5%, 1%, and 2 %). The addition of Al_2O_3 would enhance Nusselt number by 15, 14, 11 % respectively to pure water at low ranges of Richardson number (Ri = 0.016, ϕ = 2 %).
- Al_2O_3 nanofluid has the best average performance evaluation criteria equal to 18.2 % over TiO_2 and Cu with performance evaluation criteria of 13.5% and 10% respectively.
- The augmentation of the friction effect of hybrid nanofluids is far more remarkable than the contribution to heat transfer enhancement.
- The inclusion of nanoparticles in ionic fluids with different concentrations (0.5%, 1%, and 2.5%) has positively affected the Nusselt number compared to its base fluid. However, increasing nanoparticle concentration (ϕ = 2.5 %) comes with a high penalty of friction coefficient and pressure drop.
- Ionic nanofluids are highly recommended for applications with a high focus on the enhancement of heat transfer without greatly considering the pressure drop.

- Nanofluids are strongly advised with applications seeking heat transfer development having a lower increase in the friction effect.

Declaration of Competing Interest

The authors declare that they have no known competing financial interests or personal relationships that could have appeared to influence the work reported in this paper.

References

[1] P.K. Das, A review based on the effect and mechanism of thermal conductivity of normal nanofluids and hybrid nanofluids, J. Mol. Liq. 240 (2017) 420–446.

[2] Q. Xiong, S. Altnji, T. Tayebi, M. Izadi, A. Hajjar, B. Sundén, L.K.B. Li, A comprehensive review on the application of hybrid nanofluids in solar energy collectors, Sustainable Energy Technol. Assess. 47 (2021) 101341, https://doi.org/10.1016/j.seta.2021.101341.

[3] M. Ghalambaz, M.A. Sheremet, I. Pop, X.-D. Wang, Free convection in a parallelogrammic porous cavity filled with a nanofluid using Tiwari and Das' nanofluid model, PLoS ONE 10 (5) (2015) e0126486.

[4] J.H. Lee, Convection performance of nanofluids for electronics cooling, Stanford University, 2009.

[5] K. Bashirnezhad, M. Ghavami, A.A.A.A. Alrashed, Experimental investigations of nanofluids convective heat transfer in different flow regimes: A review, J. Mol. Liq. 244 (2017) 309–321.

[6] H. Babar, H.M. Ali, Towards hybrid nanofluids: Preparation, thermophysical properties, applications, and challenges, J. Mol. Liq. 281 (2019) 598–633.

[7] F. Abbas, H.M. Ali, T.R. Shah, H. Babar, M.M. Janjua, U. Sajjad, M. Amer, Nanofluid: Potential evaluation in automotive radiator, J. Mol. Liq. 297 (2020) 112014, https://doi.org/10.1016/j.molliq.2019.112014.

[8] S.K. Singh, A.W. Savoy, Ionic liquids synthesis and applications: An overview, J. Mol. Liq. 297 (2020) 112038, https://doi.org/10.1016/j.molliq.2019.112038.

[9] B. Bakthavatchalam, K. Habib, R. Saidur, B.B. Saha, K. Irshad, Comprehensive study on nanofluid and ionanofluid for heat transfer enhancement: A review on current and future perspective, J. Mol. Liq. 305 (2020) 112787, https://doi.org/10.1016/j.molliq.2020.112787.

[10] S. Lee, S.-S. Choi, S. Li, and, and J. J. J. o. H. t. Eastman, "Measuring thermal conductivity of fluids containing oxide nanoparticles," vol. 121, pp. 280–289, 1999.

[11] X. Wang, X. Xu, S. U. J. J. o. t. S. Choi, and h. transfer, "Thermal conductivity of nanoparticle-fluid mixture," vol. 13, pp. 474–480, 1999.

[12] D. Wen, Y. Ding, Experimental investigation into convective heat transfer of nanofluids at the entrance region under laminar flow conditions, Int. J. Heat Mass Transf. 47 (2004) 5181–5188.

[13] E. Esmaeilzadeh, H. Almohammadi, S.h. Nasiri Vatan, A.N. Omrani, Experimental investigation of hydrodynamics and heat transfer characteristics of γ-Al2O3/water under laminar flow inside a horizontal tube, Int. J. Therm. Sci. 63 (2013) 31–37.

[14] L. Colla, L. Fedele, M.H. Buschmann, Laminar mixed convection of TiO_2 –water nanofluid in horizontal uniformly heated pipe flow, Int. J. Therm. Sci. 97 (2015) 26–40.

[15] S. Suresh, K.P. Venkitaraj, P. Selvakumar, M. Chandrasekar, Synthesis of Al_2O_3–Cu/water hybrid nanofluids using two step method and its thermo physical properties, Colloids Surf., A 388 (1-3) (2011) 41–48.

[16] S. Suresh, K.P. Venkitaraj, P. Selvakumar, M. Chandrasekar, Effect of Al_2O_3–Cu/water hybrid nanofluid in heat transfer, Exp. Therm Fluid Sci. 38 (2012) 54–60.

[17] A.A. Minea, Challenges in hybrid nanofluids behavior in turbulent flow: Recent research and numerical comparison, Renew. Sustain. Energy Rev. 71 (2017) 426–434.

[18] A.A. Minea, W.M. El-Maghlany, Influence of hybrid nanofluids on the performance of parabolic trough collectors in solar thermal systems: Recent findings and numerical comparison, Renewable Energy 120 (2018) 350–364.

[19] H. Xie, Z. Zhao, J. Zhao, H. Gao, Measurement of thermal conductivity, viscosity and density of ionic liquid [EMIM][DEP]-based nanofluids, Chin. J. Chem. Eng. 24 (3) (2016) 331–338.

[20] A.-A. Minea, W.M. El-Maghlany, Natural convection heat transfer utilizing ionic nanofluids with temperature-dependent thermophysical properties, Chem. Eng. Sci. 174 (2017) 13–24.

[21] A.A. Minea, S.M.S. Murshed, A review on development of ionic liquid based nanofluids and their heat transfer behavior, Renew. Sustain. Energy Rev. 91 (2018) 584–599.

[22] Z.-Z. Feng, W. Li, Laminar mixed convection of large-Prandtl-number in-tube nanofluid flow, Part I: Experimental study, Int. J. Heat Mass Transf. 65 (2013) 919–927.

[23] W. Li, Z.-Z. Feng, Laminar mixed convection of large-Prandtl-number in-tube nanofluid flow, Part II: Correlations, Int. J. Heat Mass Transf. 65 (2013) 928–935.

[24] R. Ben Mansour, N. Galanis, C.T. Nguyen, Experimental study of mixed convection with water–Al2O3 nanofluid in inclined tube with uniform wall heat flux, Int. J. Therm. Sci. 50 (2011) 403–410.

[25] R. Ben Mansour, N. Galanis, C.T. Nguyen, Developing laminar mixed convection of nanofluids in an inclined tube with uniform wall heat flux, Int. J. Numer. Meth. Heat Fluid Flow 19 (2009) 146–164.

[26] S.P. Jang, S.U.S. Choi, Role of Brownian motion in the enhanced thermal conductivity of nanofluids 84 (2004) 4316–4318.

[27] R. Prasher, P. Bhattacharya, and P. E. Phelan, "Thermal Conductivity of Nanoscale Colloidal Solutions (Nanofluids)," *Physical Review Letters,* vol. 94, p. 025901, 01/18/ 2005.

[28] P. Keblinski, S.R. Phillpot, S.U.S. Choi, J.A. Eastman, Mechanisms of heat flow in suspensions of nano-sized particles (nanofluids), Int. J. Heat Mass Transf. 45 (2002/02/01/ 2002.) 855–863.

[29] C.H. Li, G.P. Peterson, "Dual Role of Nanoparticles in the Thermal Conductivity Enhancement of Nanoparticle Suspensions," in *ASME*, Int. Mech. Eng. Congress Exposition 2005 (2005) 745–750.

[30] O. Mahian, L. Kolsi, M. Amani, P. Estellé, G. Ahmadi, C. Kleinstreuer, et al, Recent advances in modeling and simulation of nanofluid flows—Part II: Applications, Phys. Rep. 791 (2019/02/13/ 2019.) 1–59.

[31] O. Mahian, L. Kolsi, M. Amani, P. Estellé, G. Ahmadi, C. Kleinstreuer, et al, Recent advances in modeling and simulation of nanofluid flows-Part I: Fundamentals and theory, Phys. Rep. 790 (2019/02/03/ 2019.) 1–48.

[32] J. C. Maxwell, "A Treatise on Electricity and Magnetism," *Oxford University,* vol. vol. 1, 1872.

[33] H.J. Jouybari, S. Saedodin, A. Zamzamian, M.E. Nimvari, S. Wongwises, Effects of porous material and nanoparticles on the thermal performance of a flat plate solar collector: An experimental study, Renew. Energy 114 (2017) 1407–1418.

[34] H.J. Xu, Z.B. Xing, F.Q. Wang, Z.M. Cheng, Review on heat conduction, heat convection, thermal radiation and phase change heat transfer of nanofluids in porous media: Fundamentals and applications, Chem. Eng. Sci. 195 (2019) 462–483.

[35] A.A.R. Darzi, M. Farhadi, K. Sedighi, Heat transfer and flow characteristics of AL2O3–water nanofluid in a double tube heat exchanger, Int. Commun. Heat Mass Transfer 47 (2013/10/01/ 2013.) 105–112.
[36] S. Patankar, Numerical heat transfer and fluid flow, CRC Press, 1980.
[37] B. Ghasemi, S. Aminossadati, Periodic natural convection in a nanofluid-filled enclosure with oscillating heat flux, Int. J. Therm. Sci. 49 (2010) 1–9.
[38] S.A.M. Mehryan, F.M. Kashkooli, M. Ghalambaz, A.J. Chamkha, Free convection of hybrid Al 2 O 3 -Cu water nanofluid in a differentially heated porous cavity, Adv. Powder Technol. 28 (2017) 2295–2305.
[39] T.C. Paul, A.K.M.M. Morshed, E.B. Fox, J.A. Khan, Thermal performance of Al2O3 Nanoparticle Enhanced Ionic Liquids (NEILs) for Concentrated Solar Power (CSP) applications, Int. J. Heat Mass Transf. 85 (2015) 585–594.
[40] A.M. Hussein, M.M. Noor, K. Kadirgama, D. Ramasamy, M. M. Rahman, Heat transfer enhancement using hybrid nanoparticles in ethylene glycol through a horizontal heated tube, Int. J. Autom. Mech. Eng. 14 (2017) 4183–4195.
[41] F. Hekmatipour, M.A. Akhavan-Behabadi, B. Sajadi, Combined free and forced convection heat transfer of the copper oxide-heat transfer oil (CuO-HTO) nanofluid inside horizontal tubes under constant wall temperature, Appl. Therm. Eng. 100 (2016) 621–627.